TRANSITION FROM ANNULAR FLOW AND FROM DISPERSED BUBBLE FLOW—UNIFIED MODELS FOR THE WHOLE RANGE OF PIPE INCLINATIONS

D. BARNEA

Department of Fluid Mechanics and Heat Transfer, Tel-Aviv University, Ramat-Aviv 69978, Israel

Abstract—New models are suggested for the transition from annular to intermittent flow and from dispersed bubble flow for two-phase gas–liquid flow in inclined pipes. The models display a smooth change in mechanisms as the pipe inclination varies over the whole range of upward and downward inclinations. The results of the models compare favorably with experimental data.

INTRODUCTION

The prediction of flow patterns in gas–liquid flow in pipes is one of the most important problems in two-phase flow. Traditionally, the approach that has been used to treat this problem was to correlate the data and to plot the results on a "flow-pattern map". A wide variety of maps with different coordinate systems have been published.

Recently, efforts were directed towards the development of physical models that allow the analytical prediction of the flow patterns and the transition boundaries. Such an approach was used by Taitel & Dukler (1976) for horizontal and slightly inclined flow, Taitel *et al.* (1980) and Mishima & Ishii (1981) for the case of vertical upward flow, and Barnea *et al.* (1982a) for vertical downward flow.

Physical models for flow-pattern transitions in inclined pipes were presented by Barnea *et al.* (1982b) for downward inclinations and Barnea *et al.* (1985) for upward inclinations. The approach taken was to extend and modify the vertical models to include steep inclinations, while the shallow inclinations were treated via an extension of the horizontal case.

In the development of predictive models for flow-pattern transition boundaries the objective should be to propose models that will apply to all angles of inclination, i.e. that the effect of inclination will be incorporated in the model in such a way that the same model will apply for horizontal, vertical upward, vertical downward and all angles of inclination.

So far this aim has not been fully achieved in the models presented by Barnea *et al.* (1982b, 1985). The main disadvantage in these models arises when dealing with the transition from annular to intermittent flow and the transition from the dispersed bubble flow. These two transition boundaries exist in the whole range of inclinations (although not necessarily at the same location on the flow-pattern map), but different mechanisms were suggested for these two boundaries in the horizontal (Taitel & Dukler 1976) and vertical (Taitel *et al.* 1980; Barnea *et al.* 1982a) cases.

Transition to annular flow according to the "horizontal" model of Taitel & Dukler (1976), requires that stratified flow becomes unstable while the liquid level is low enough to form an annular film rather than a complete bridge that leads to slug flow. For the upward vertical case, Taitel *et al.* (1980) suggested a totally different mechanism for the transition to annular flow. In this case the gas velocity must be large enough to lift the largest stable drop in order to maintain annular flow. The "downward vertical" model, presented by Barnea *et al.* (1982a), adopted the same idea as the "horizontal" model and suggests that the transition from annular to intermittent flow occurs when the liquid holdup is large enough to cause a blockage of the gas core.

The transition to dispersed bubbles was determined from a balance between breakage

forces due to turbulence and coalescence forces due to gravity in the "horizontal" model or due to surface tension in the "vertical" models.

The effect of shallow inclinations from the horizontal on the transitions to dispersed bubble and annular flows has already been incorporated in the "horizontal" model by Taitel & Dukler (1976). In a similar way, the mechanisms presented in the "vertical" models were modified for slight changes from the vertical (Barnea et al. 1982b, 1985). Since the transition mechanisms for the horizontal and shallow inclinations differ from those of vertical and steep inclinations, it is necessary to choose the appropriate mechanism in intermediate angles of inclination, and thus to determine the applicability of the shallow and steep-inclination models.

The terms shallow and steep inclination may thus apply to different inclination angles for each transition boundary. In addition the "switch" between the two mechanisms was based on experimental results in an air–water system.

In this work new models are suggested for the transition from annular to intermittent flow and from dispersed bubble flow, in which the effect of inclination is integratively incorporated in the models. In fact, the same transition criteria apply for the whole range of inclinations and the problem of switching between two different mechanisms and selecting the applicable one, is thus eliminated.

TRANSITION FROM ANNULAR TO INTERMITTENT FLOW

In annular flow the gas flows along the center of the tube and the liquid flows as a film around the tube walls. Transition from annular to intermittent flow will occur when this characteristic structure is destroyed by occasional blocking of the gas core by liquid lumps.

Figure 1 shows the geometry of annular film flow in an inclined pipe. A force balance for steady annular flow gives:

for the liquid film

$$-A_L \frac{dp}{dz} - \tau_L S_L + \tau_i S_i - \rho_L A_L g \sin \beta = 0 \qquad [1]$$

and

for the gas core

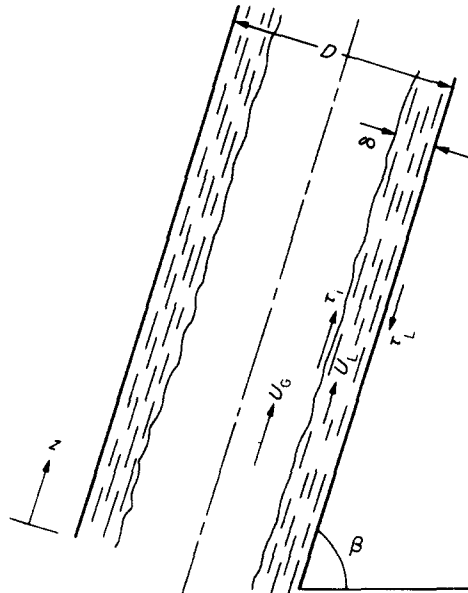$$-A_G \frac{dp}{dz} - \tau_i S_i - \rho_G A_G g \sin \beta = 0, \qquad [2]$$

Figure 1. Geometry of annular flow.

where τ_L is the shear stress at the wall, τ_i is the interfacial stress, A_L and A_G are the cross-sectional areas occupied by the liquid and gas, respectively, S_L and S_i are the perimeters over which τ_L and τ_i act, respectively, ρ_L and ρ_G are the liquid and gas densities, respectively, z is the axial coordinate, p is the static pressure, β is the angle of inclination from the horizontal and g is the acceleration due to gravity.

Equating the pressure drop in the two phases yields the following result:

$$\tau_i S_i \left(\frac{1}{A_L} + \frac{1}{A_G}\right) - g\,(\rho_L - \rho_G)\sin\beta - \tau_L \frac{S_L}{A_L} = 0, \qquad [3]$$

where β is positive for upward flow and negative for downward flow.

The shear stress τ_L is related to the liquid average axial velocity U_L by

$$\tau_L = f_L \frac{\rho_L U_L^2}{2}, \qquad [4]$$

with the liquid/wall friction factor f_L evaluated from

$$f_L = C_L \left(\frac{D_L U_L}{\nu_L}\right)^{-n}, \qquad [5]$$

where $D_L = 4A_L/S_L$ is the hydraulic diameter, ν_L is the liquid kinematic viscosity and C_L and n are constants in the friction factor correlation.

The film flow geometry is given in terms of the film thickness δ and the tube diameter D:

$$\left.\begin{array}{l} S_L = \pi D, \quad S_i = \pi(D - 2\delta) \\[2mm] A_L = \pi\,(D\delta - \delta^2) \quad \text{and} \quad A_G = \pi\left(\frac{D}{2} - \delta\right)^2. \end{array}\right\} \qquad [6]$$

Substituting in [3] and rearranging yields

$$\tau_i = g\,(\rho_L - \rho_G)\,D\,\sin\beta\,(\tilde{\delta} - \tilde{\delta}^2)(1 - 2\tilde{\delta}) + \tfrac{1}{32}\,C_L\,\rho_L\left(\frac{D}{\nu_L}\right)^{-n}(U_{LS})^{2-n}\left[\frac{(1 - 2\tilde{\delta})}{(\tilde{\delta} - \tilde{\delta}^2)^2}\right], \qquad [7]$$

where U_{LS} is the liquid superficial velocity and $\tilde{\delta}$ the dimensionless film thickness $(\tilde{\delta} = \delta/D)$.

In this work the following coefficients were used: $C_L = 0.046$, $n = 0.2$ for a turbulent liquid film and $C_L = 16$, $n = 1.0$ for laminar flow in the film.

Equation [7] relates the interfacial shear τ_i to the film thickness $\tilde{\delta}$ for a constant value of the liquid superficial velocity U_{LS}. This relation for vertical upward flow is shown by the solid lines in figure 2 for different values of U_{LS}. The interfacial shear τ_i is provided by the gas flow rate. The basic mechanisms which determine the interfacial shear are not fully understood and the available relationships are largely empirical. Wallis (1968) correlated a variety of data for annular cocurrent flow by the simple relation for the interfacial friction factor:

$$f_i = f_G(1 + 300\,\tilde{\delta}), \qquad [8]$$

where f_G is the friction factor in the absence of the film, namely

$$f_G = C_G \left(\frac{U_{GS} D}{\nu_G}\right)^{-m}. \qquad [9]$$

Thus, the equation

$$\tau_i = \tfrac{1}{2} f_i\,\rho_G \frac{U_{GS}^2}{(1 - 2\tilde{\delta})^4} \qquad [10]$$

yields the required relationship between the interfacial shear stress and the gas flow rate, where ν_G is the gas kinematic viscosity and U_{GS} is the superficial gas velocity.
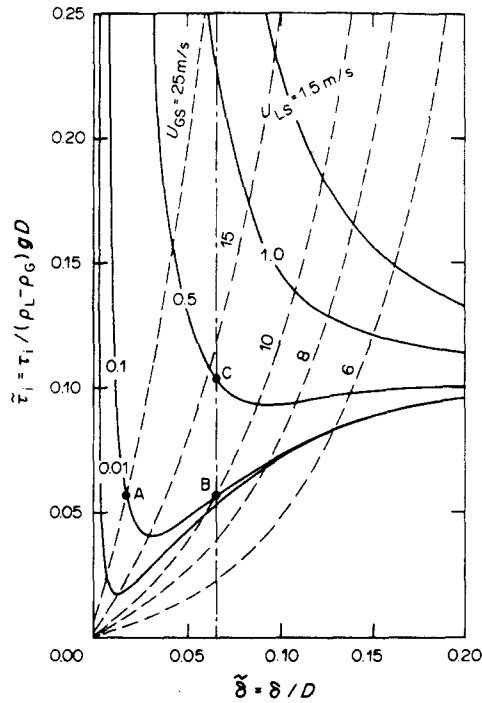
Figure 2. Steady-state solutions for vertical annular flow. Air–water, 0.1 MPa, 25°C, 2.5 cm dia.
———, [7]; — — —, [10]; — — — —, [12].

This independent expression for τ_i is given by the broken curves in figure 2. Any intersection of the solid and the broken curves yields a steady-state solution for annular flow at a particular flow rate of liquid and gas.

As mentioned above, transition from annular to intermittent flow occurs when the gas core is blocked at any location by the liquid. Blockage of the core may result from two possible mechanisms:

(a) instability of annular flow that prevents a stable annular configuration;

(b) the liquid film being large enough to cause spontaneous blockage as a result of axial transfer of liquid in the film.

The stability criterion [mechanism (a)]

In figure 2, curves of $\tilde{\tau}_i [\tilde{\tau}_i = \tau_i/(\rho_L - \rho_G)gD]$ vs $\tilde{\delta}$ are presented for vertical upward flow. The solid lines are plots of [7] (for parametric values of U_{LS}) which result from momentum balances, and the broken curves give the relationship between $\tilde{\tau}_i$ and $\tilde{\delta}$ for different gas flow rates as dictated by [10]. The curves represented by the solid lines display a minimum. Barnea & Taitel (1985) showed that this minimum is associated with the change in the direction of the velocity profile in the film. The branch to the left of the minimum corresponds to stable steady-state solutions with positive velocity profiles (point A). The right-hand branch corresponds to solutions with a negative velocity profile near the wall (point B). Thus, solutions to the right of the minimum are unstable, the liquid near the wall that flows downwards accumulates at the pipe entrance causing a blockage of the air passage and transition to intermittent flow. Note that in the case of countercurrent flow this minimum is equivalent to the point of flow reversal (Taitel *et al.* 1982; Barnea & Taitel 1985). The point of intersection at the minimum represents the locus where transition from stable annular flow to intermittent flow occurs.

For any given U_{LS}, the film thickness at the minimum is obtained by differentiating [7]

with respect to δ and equating it to zero, which yields

$$g\,(\rho_L - \rho_G)D \sin\beta[(1 - 2\delta)^2 - 2(\delta - \delta^2)]$$

$$-\tfrac{1}{16}C_L\rho_L\left(\frac{D}{\nu_L}\right)^{-n}(U_{LS})^{2-n}\left[\frac{(\delta - \delta^2) + (1 - 2\delta)^2}{(\delta - \delta^2)^3}\right] = 0. \quad [11]$$

A simultaneous solution of [7] and [10] with δ that satisfies [11] ($\delta = \delta_{min}$) yields the value of U_{GS} at the transition. The locus of the flow rate pairs at the minimum represents the condition of neutral stability where transition from annular to intermittent flow occurs.

The spontaneous blockage criterion [mechanism (b)]

Blockage of the gas core in annular flow may also occur when the supply of liquid in the film is large enough to provide the liquid needed to maintain a liquid bridge. Owing to the presence of waves on the interface fluid is transferred axially from the wave trough to the wave crest. When sufficient liquid is accumulated at the crest the pipe is bridged and transition to intermittent flow occurs.

Based on this mechanism, Barnea et al. (1982a) suggested that intermittent flow will develop when

$$\frac{A_L}{A\,R_{sm}} = \frac{\alpha_L}{R_{sm}} \geqslant 0.5, \quad [12]$$

where A is the pipe cross-sectional area and R_{sm} is the minimal liquid holdup within the formed liquid bridge that will allow competent blockage of the gas passage. This minimum value is related to the maximum bubble volumetric packing in the liquid slug and equals approx. 0.48 (Barnea & Brauner 1985). Lower values of R_s will make slugging impossible due to the high gas void fraction. This value of R_{sm} is not necessarily the actual equilibrium liquid holdup, R_s, within the fully-developed slug near the transition boundary [the method for predicting this equilibrium value of R_s has been proposed by Barnea & Brauner (1985)]. Note, however that the minimal value of R_{sm} in [12] is equal to the actual R_s on the annular–intermittent transition boundary in a very wide range of flow conditions.

The combined criterion

Consider, for example, stable annular flow as represented by point A in figure 2. Decreasing the gas flow rate while maintaining U_{LS} constant causes the intersection points of the steady-state solutions to move along the stable branch on the solid curve towards higher values of the film thickness δ. If the minimum is reached before the condition of $A_L/A = 0.5\,R_{sm}$ is satisfied, transition to slug flow occurs owing to mechanism (a). There are, however, cases where the film thickness along the stable branch (before the minimum is reached) is large enough to cause blockage according to mechanism (b) (point C), and thus transition to slug flow occurs even before the condition of instability is reached.

Referring to figure 2, it can be seen that as the liquid flow rate increases the location of the minimum is shifted to the right, namely towards higher values of δ. As a result, transition to slug flow at low liquid flow rates occurs owing to film instability [mechanism (a)], while at high values of U_{LS} transition takes place due to a very high liquid holdup [mechanism (b)].

Effect of pipe inclination

Curves of $\tilde{\tau}_i$ vs δ ([7]) are shown in figure 3 for the whole range of pipe inclinations. When the pipe is declined from the vertical the minimum, which separates the stable and unstable branches, is shifted towards higher values of δ, and for high liquid flow rates the minimum is not seen at all. For the case of horizontal and downward inclinations, [7] does not display any minimum for all values of U_{LS}, the solution is always stable, and thus transition from annular to slug flow occurs only according to mechanism (b) in the whole range of flow rates.
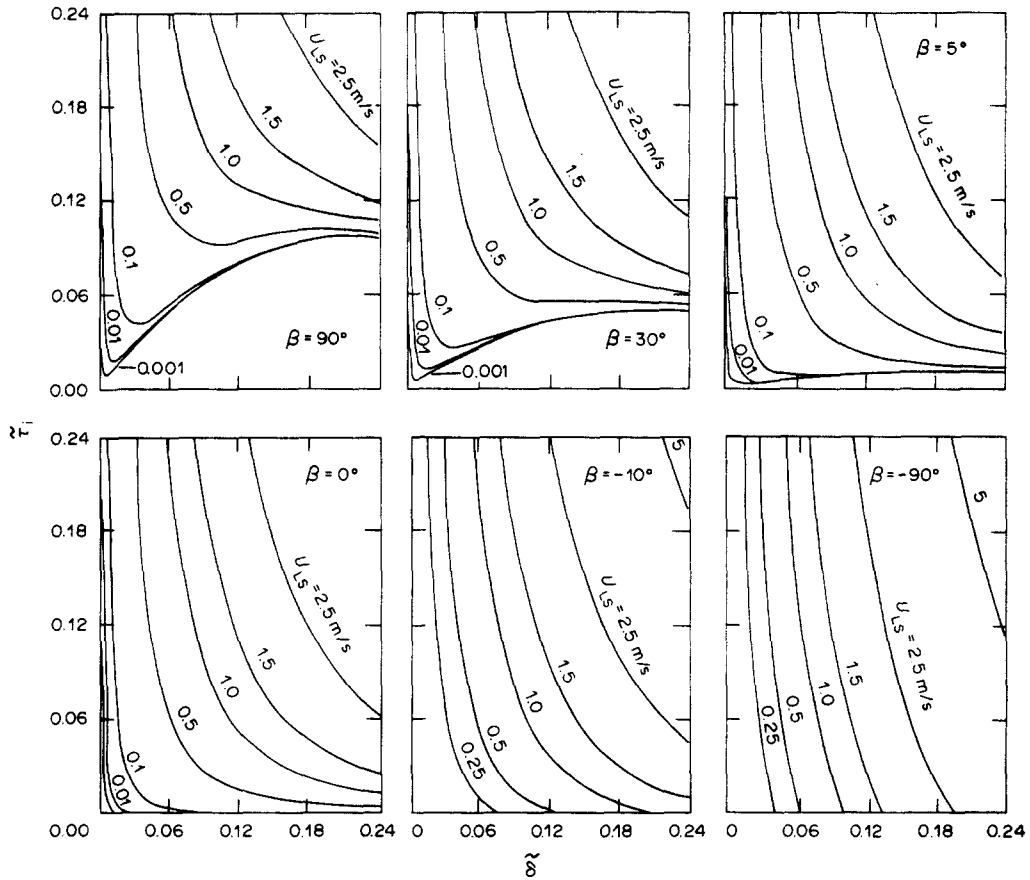
Figure 3. Effect of inclination on the stable branch. Air–water, 0.1 MPa, 25°C, 2.5 cm dia.

In vertical upward flow the two mechanisms (a) and (b) play a role in the transition to slug flow. As the pipe is declined from the vertical the transition due to the film instability [transition (a)] is confined to very low liquid flow rates until it disappears at horizontal and downward flow, where the only mechanism that determines the transition to slug flow is the blockage mechanism (b).

The two mechanisms (a) and (b) mentioned above are both based on the characteristic film structure of annular flow. A smooth change in mechanisms is obtained as the pipe inclination varies over all possible angles and thus the transition from annular to intermittent flow is applicable in the whole range of inclinations.

Transition boundaries between annular and intermittent flow based on the above concept are plotted in figure 4 and show good agreement with experimental data taken for air–water in a 2.5 cm dia pipe. Note that the transition lines may be terminated by the stratified/nonstratified transition line, which can be predicted by the Taitel & Dukler (1976) and Barnea et al. (1982b) methods. Thus, the above-proposed model is applicable only outside the range of stable stratified flow.

The predicted transition boundaries are also compared with data for a Freon-113 vapor–liquid system (Weisman et al. 1979; Weisman & Kang 1981). Figure 5 shows the results for three pipe positions: horizontal, 45° upward inclination and vertical upward flow. The theoretical transition lines are in good agreement with the experimental data for 45° and 90° upward inclination. The discrepancy observed for the case of $\beta = 0$ (the dotted region) is probably related to the wavy annular pattern (Barnea et al. 1980) which may be easily interpreted as stratified wavy flow or slug flow. Note also, that Weisman's data for air–water show a similar discrepancy from the present model as well as from Shoham's (1982) experimental data (figure 4, $\beta = 0$). Clearly this conflict invites future clarification of this particular transition line in horizontal and slightly inclined pipes.
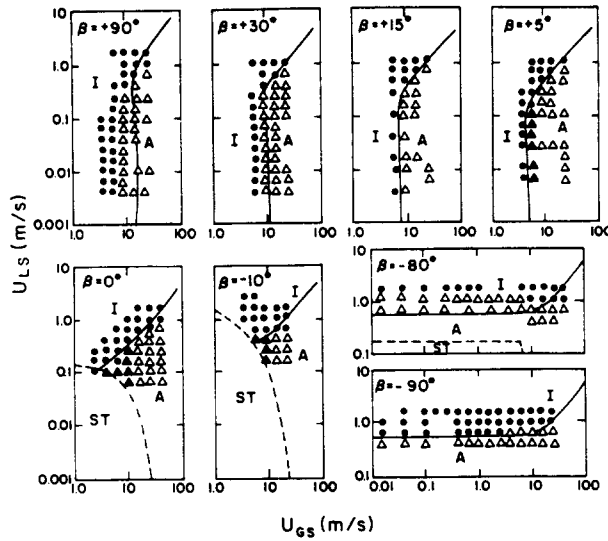
Figure 4. Annular/intermittent transition. Air–water, 0.1 MPa, 25°C, 2.5 cm dia. ——, Theory; ---, Taitel & Dukler model (1976); data (Shoham 1982): $\triangle$ annular and $\blacktriangle$ wavy annular (A); $\bullet$ slug and $\ominus$ churn (I).

The dimensionless form of the transition criteria

For convenience, the aforementioned procedure can be written in general dimensionless form. The solution for the steady-state liquid holdup α_L (or film thickness) in annular flow, given by [7] and [10], yields

$$Y = \frac{1 + 75\alpha_L}{(1 - \alpha_L)^{\frac{5}{2}}\alpha_L} - \frac{1}{\alpha_L^3} X^2,$$ [13]

where

$$X^2 = \frac{\dfrac{4C_L}{D}\left(\dfrac{U_{LS}D}{v_L}\right)^{-n}\dfrac{\rho_L U_{LS}}{2}}{\dfrac{4C_G}{D}\left(\dfrac{U_{GS}D}{v_G}\right)^{-m}\dfrac{\rho_G U_{GS}}{2}} = \frac{\left(\dfrac{dp}{dz}\right)_{LS}}{\left(\dfrac{dp}{dz}\right)_{GS}}$$

and

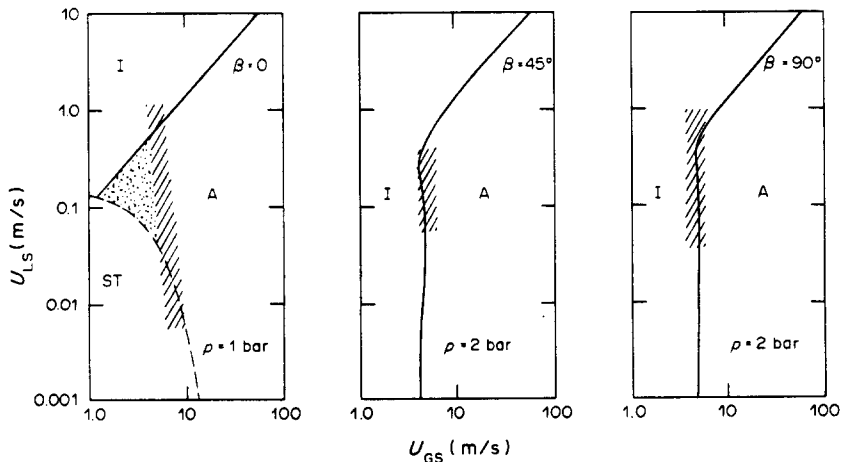$$Y = \frac{(\rho_L - \rho_G)g \sin \beta}{\left(\dfrac{dp}{dz}\right)_{GS}}.$$ [14]

Figure 5. Annular/intermittent transition. Freon-113, 2.5 cm dia. ——, Theory; ---, Taitel & Dukler model (1976); //////, experimental boundary (Weisman *et al.* 1979; Weisman & Kang 1981).
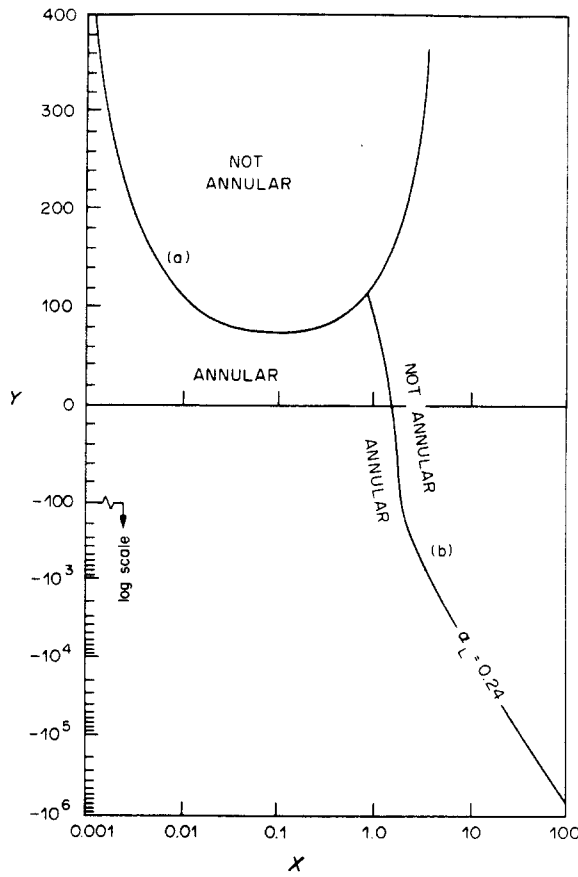
Figure 6. Generalized map for annular/intermittent transition.

Note also that

$$\alpha_L = 4\,(\tilde{\delta} - \tilde{\delta}^2)$$

and

$$\alpha_G = 1 - \alpha_L = (1 - 2\tilde{\delta})^2.$$

[15]

Equation [11], which yields the condition for the minimum $\tilde{\tau}_i$ along a line of constant U_{LS}, can be written in the form

$$Y = \frac{2 - \frac{3}{2}\alpha_L}{\alpha_L^3\,(1 - \frac{3}{2}\alpha_L)}\,X^2.$$

[16]

The transition boundaries can thus be plotted on a generalized map using X and Y as dimensionless coordinates (figure 6). Simultaneous solution of [13] and [16] yields the locus of (X, Y) pairs [line (a)] along the neutral stability curve [transition mechanism (a)]. The region below this curve is in stable annular flow, while the region above it yields unstable conditions or intermittent flow.

Equation [13], with the value of $\alpha_L = 0.5R_{sm}$ yields the condition where blockage occurs [mechanism (b)]. Equation [13] is plotted for a constant value of $\alpha_L = 0.24$ ($R_{sm} = 0.48$) within the stable zone [line (b)]. The region to the left of curve (b) corresponds to annular flow.

TRANSITION FROM DISPERSED BUBBLES

The mechanism of transition from dispersed bubbles to slug flow suggested for vertical flows (Taitel *et al.* 1980; Barnea *et al.* 1982a) is based on the concept that turbulent forces

overcome interfacial tension to dispersed the gas phase into small bubbles. Based on Hinze's (1955) results for the characteristic size of bubbles in a dispersion at low concentration of the dispersed phase, and Calderbank's (1958) investigation on the effect of the gas holdup on the resulting bubble size, Barnea et al. (1982a) suggested the following relation for the stable diameter of the dispersed bubbles:

$$d_{\text{max}} = (0.725 + 4.15\, \alpha^{\frac{1}{2}}) \left(\frac{\sigma}{\rho_{\text{L}}}\right)^{\frac{3}{5}} \epsilon^{-\frac{2}{5}}, \qquad [17]$$

where α is the dispersed bubbles void fraction ($\alpha = U_{\text{GS}}/U_{\text{M}}$) and ϵ is the rate of energy dissipation per unit mass. For turbulent pipe flow,

$$\epsilon = \frac{2f_{\text{M}}}{D} U_{\text{M}}^3, \qquad [18]$$

where U_{M} is the mixture velocity ($U_{\text{M}} = U_{\text{LS}} + U_{\text{GS}}$) and f_{M} is the friction factor based on the mixture velocity.

Equation [17] is applicable only to the dispersed bubble regime. In this regime the bubble size is small enough to prevent deformation, and thus to prevent agglomeration and coalescence. When the bubble size is large enough to cause distortion from the spherical shape, coalescence is enchanced and transition from dispersed bubble flow takes place. This critical bubble size was estimated as the one above which the bubble is deformed and the rise velocity is constant (Barnea et al. 1982a):

$$d_{\text{CD}} = 2 \left[\frac{0.4\sigma}{(\rho_{\text{L}} - \rho_{\text{G}})g}\right]^{\frac{1}{2}}. \qquad [19]$$

Substituting d_{CD} for d_{max} in [17] yields the transition boundary from the dispersed bubble regime.

For horizontal and slightly inclined flow Taitel & Dukler (1976) suggested that the transition to dispersed bubble flow takes place when the turbulent fluctuations overcome the buoyant forces. The turbulent and buoyant forces were evaluated per unit length of the gas and liquid in stratified flow. This mechanism predicts quite well the transition to dispersed bubble flow in horizontal and slightly inclined pipes, but fails to predict this transition when the angle of inclination deviates considerably from the horizontal.

In this work the effect of buoyancy is revised to act on a single bubble. It is suggested that transition from dispersed bubble flow takes place either as a result of:

(a) Agglomeration of large distorted bubbles
or
(b) migration of bubbles, due to buoyancy, to the upper part of the pipe (creaming).

The transition that corresponds to (a) is obtained when d_{max} in [17] is equated with d_{CD} in [19]. Mechanism (b) takes place when the critical bubble size d_{CB} is large enough to cause creaming.

This critical bubble size can be estimated as follows. Consider fully dispersed bubble flow in an inclined pipe (figure 7). The forces that act on a dispersed bubble are the buoyancy which tends to lift the dispersed bubble to the upper part of the pipe and enhance the transition to intermittent flow, and the turbulence which tends to disperse the bubble and to maintain the dispersed bubble pattern. The balance between these forces yields the critical bubble diameter for "creaming".

The buoyancy component in the radial direction is

$$F_{\text{B}} = (\rho_{\text{L}} - \rho_{\text{G}})g \cos \beta \frac{\pi d^3}{6}. \qquad [20]$$
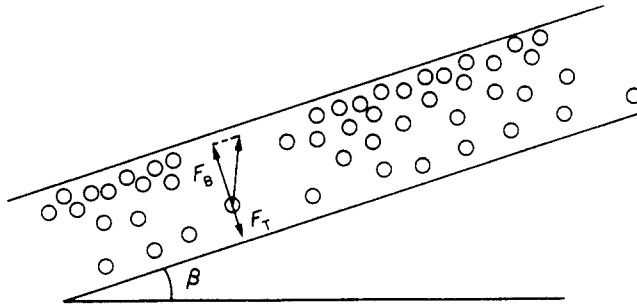
Figure 7. Forces on a bubble in dispersed bubble flow.

The force acting due to turbulent fluctuations (Levich 1962) is

$$F_T = \tfrac{1}{2} \rho_L v'^2 \frac{\pi d^2}{4},$$ [21]

where v' is the radial velocity fluctuations whose r.m.s. is estimated to be approximately equal to the friction velocity, U_*. Thus,

$$\overline{(v'^2)}^{\frac{1}{2}} = U_* = U_M \left(\frac{f_M}{2}\right)^{\frac{1}{2}}.$$ [22]

Migration of dispersed bubbles towards the upper pipe wall takes place when

$$F_B > F_T$$

or

$$d > d_{CB} = \frac{3}{8} \frac{\rho_L}{(\rho_L - \rho_G)} \frac{f_M U_M^2}{g \cos\beta}.$$ [23]

In order to maintain dispersed bubble flow, neither distortion of the bubble, nor creaming should take place. It means that d_{max} should be less then d_{CD} as well as d_{CB}. Thus the bubble diameter d_{max} [17] that determines transition is the smallest of d_{CD} or d_{CB}. The transition line, [17] with $d_{max} = d_{CD}$, is shown by the solid line in figure 8, while [17] with $d_{max} = d_{CB}$ is marked by the broken curve. The combined transition boundary is shown by the thicker sections of the curves (the outer envelope). Note that d_{CB} is smallest in the horizontal and increases as the angle of inclination increases. For an air–water system d_{CB} in horizontal and moderate inclincations is smaller than d_{CD}, yielding transitions at higher mixture velocities than those predicted by d_{CD}, while for steep inclinations and vertical flows d_{CD} is smaller and the effect of buoyancy on the transition from dispersed bubbles is ignored. Note that this transition boundary [17] is valid for gas void fractions <0.52. At $\alpha = 0.52$ the maximum volumetric packing density of the bubbles is reached and coalescence to intermittent flow occurs even at high turbulence levels. The transition curve that characterizes this condition is

$$U_{LS} = U_{GS} \frac{1-\alpha}{\alpha},$$ [24]

where $\alpha = 0.52$ (Taitel et al. 1980). The theoretical transition lines from dispersed bubble flow are shown in figure 8 for the whole range of pipe inclinations and the agreement with the experimental results is satisfactory.

SUMMARY AND CONCLUSIONS

Unified models which incorporate the effect of the angle of inclination are presented for the transition from annular flow and from dispersed bubble flow. These two afore-
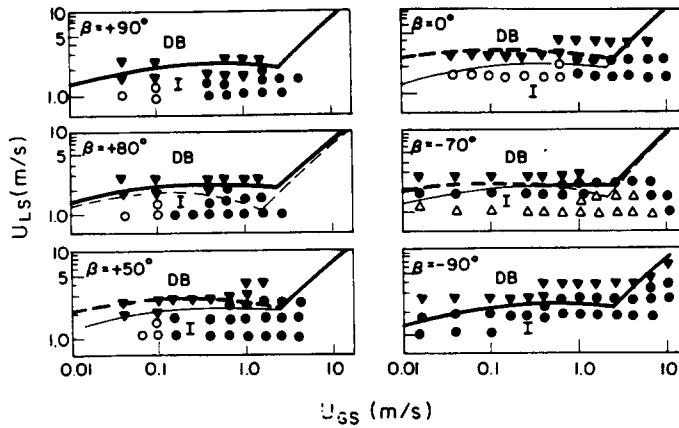
Figure 8. Transition from dispersed bubble flow. Air–water, 0.1 MPa, 25°C, 2.5 cm dia. Theory: ——— [17, 19]; – – – [17, 23]. Data (Shoham 1982): ▼ dispersed bubble (DB); ● slug and ○ elongated bubble (I).

mentioned transition boundaries were treated differently in the past for near-vertical and near-horizontal inclinations and the applicability of those models for intermediate angles was questionable.

The models proposed in the present work use the same approach for the whole range of pipe inclinations. The transition from dispersed bubbles is given by [17] where d_{max} is taken as smallest between d_{CD} [19] and d_{CB} [23] and by [24] for $\alpha > 0.52$.

The transition from annular flow is given by a generalized map (figure 6) which includes the effect of inclination. The transition lines are given in terms of the dimensionless coordinates X and Y (defined by [14]). Line (a) corresponds to the instability mechanism and line (b) to the blockage mechanism. Note that the annular/intermittent transition boundary may be terminated by the stratified/nonstratified transition (figure 4). Therefore the region below (a) and to the left of (b) (figure 6) may also contain stratified flow, primarily for horizontal and downward flow. Thus, the predicted annular/intermittent boundary is applicable only outside the range of stable stratified flow (Taitel & Dukler 1976; Barnea et al. 1982b).

Acknowledgement—The author wishes to thank Professor Y. Taitel for the many useful and illuminating discussions.

REFERENCES

BARNEA, D. & BRAUNER, N. 1985 Holdup of the liquid slug in two phase intermittent flow. Int. J. Multiphase Flow 11, 43–49.

BARNEA, D. & TAITEL, Y. 1985 Stability of annular flow. Int. Commun. Heat Mass Transfer 12, 611–621.

BARNEA, D., SHOHAM, O., TAITEL, Y. & DUKLER, A. E. 1980 Flow pattern transition for gas–liquid flow in horizontal and inclined pipes. Int. J. Multiphase Flow 6, 217–225.

BARNEA, D., SHOHAM, O. & TAITEL Y. 1982a Flow pattern transition for vertical downward two phase flow. Chem. Engng Sci. 37, 741–746.

BARNEA, D., SHOHAM, O. & TAITEL, Y. 1982b Flow pattern transition for downward inclined two phase flow; horizontal to vertical. Chem. Engng Sci. 37, 735–740.

BARNEA, D., SHOHAM, O. & TAITEL, Y. 1985 Gas–liquid flow in inclined tubes: flow pattern transitions for upward flow. Chem. Engng Sci. 40, 131–136.

BRAUNER, N. & BARNEA D. 1986 Slug/churn transition in upward vertical flow. Chem. Engng Sci. 41, 159–163.

CALDERBANK, P. H. 1958 Physical rate processes in industrial fermentation; part I: the interfacial area in gas–liquid contacting with mechanical agitation. Trans. Inst. Chem. Engrs 36, 443–463.

HINZE, J. O. 1955 Fundamentals of the hydrodynamic mechanism of splitting in dispersion processes. *AIChE Jl* **1**, 289–295.

LEVICH, V. G. 1962 *Physicochemical Hydrodynamics*. Prentice-Hall, Englewood Cliffs, N.J.

MISHIMA, K. & ISHII, M. 1981 Flow regime transition criteria for two phase flow in vertical tubes. *Int. J. Heat Mass Transfer* **27**(5), 723–736.

SHOHAM, O. 1982 Flow pattern transitions and characterization in gas–liquid two phase flow in inclined pipes. Ph.D. Dissertation, Tel-Aviv Univ., Ramat-Aviv, Israel.

TAITEL, Y. & DUKLER, A. E. 1976 A model for prediction flow regime transition in horizontal and near horizontal gas–liquid flow. *AIChE Jl* **22**, 47–55.

TAITEL, Y., BARNEA, D. & DUKLER, A. E. 1980 Modeling flow pattern transitions for steady upward gas–liquid flow in vertical tubes. *AIChE Jl* **26**, 345–354.

TAITEL, Y., BARNEA, D. & DUKLER, A. E. 1982 A film model for the prediction of flooding and flow reversal for gas–liquid flow in vertical tubes. *Int. J. Multiphase Flow* **8**, 1–10.

WALLIS, G. B. 1969 *One-dimensional Two-phase Flow*. McGraw-Hill, New York.

WEISMAN, J. & KANG, S. Y. 1981 Flow pattern transitions in vertical and upwardly inclined lines. *Int. J. Multiphase Flow* **7**, 271–291.

WEISMAN, J., DUNKAN, D., GIBSON, J. & CRAWFORD, T. 1979 Effect of fluid properties and pipe diameter on two phase flow patterns in horizontal lines. *Int. J. Multiphase Flow* **5**, 437–461.